

# Formation of Network and Cellular Structures by Viscoelastic Phase Separation

By Hajime Tanaka\*

Network (sponge) and cellular structures are often seen in various types of materials. Materials with such structures are generally characterized by light weight and high mechanical strength. The usefulness of such materials is highlighted, for example, by the remarkable material properties of bone tissue, which often has a highly porous structure. In artificial materials, plastic and metallic foams and breads have such structures. Here, we describe a physical principle for producing network and cellular structures using phase separation, and its potential applications to the morphological control of materials spanning from soft to hard matter.

## 1. Introduction

Phase separation is one of the most fundamental physical phenomena that produce heterogeneous structures. Phase-separation phenomena are widely observed in various kinds of materials, such as metals, semiconductors, superconductors, simple liquids, and complex fluids, such as polymers, surfactants, colloids, emulsions, and biological materials.<sup>[1,2]</sup> The phenomena lead to pattern evolution in multicomponent mixtures of these materials and, thus, play key roles in controlling their morphology, which is related to various functions associated with mechanical, electric, and transport properties. Phase separation also plays a key role in pattern formation in nature (geological and biological pattern evolution). For example, the possible relevance of passive and active phase separation to biological systems has recently been discussed.<sup>[3,4]</sup>

Phase separation can be classified into solid- and fluid-phase separation. The former can be seen in phase separation of metallic alloys, whereas the latter can be seen, for example, in phase separation of salad dressings into oil-rich and water-rich phases. This type of phase separation can produce only two types of morphologies: a bicontinuous and a droplet structures for symmetric and asymmetric compositions, respectively. In symmetric compositions, the two coexistent phases occupy about the same volume, whereas in asymmetric compositions one of the phases occupies a much larger volume than the other. In these

types of phase separation, morphological selection is caused by minimization of the interfacial energy. For complex fluids, it is possible to produce other interesting morphologies. Nearly 20 years ago, we found a novel type of phase-separation behavior in polymer solutions,<sup>[5–10]</sup> which can be explained by neither of these models. In addition to the initial diffusive and the final hydrodynamic regimes, which are known in classical phase separation, there existed an intermediate viscoelastic regime, where elastic-force balance instead of interfacial tension determined domain morphology.

Contrary to the common sense of classical phase separation, even the minority phase transiently formed a continuous network structure. This type of phase separation is characterized by a crossover between the characteristic deformation rate induced by phase separation itself and the characteristic rheological relaxation rate of the phase rich in the slow component, which can be viewed as viscoelastic relaxation for pattern evolution (see Table 1). Thus, we named it “viscoelastic phase separation” (VPS).<sup>[7]</sup> It is worth noting that the transport mechanisms relevant to phase separation are diffusion only for solid-phase separation; diffusion and flow for fluid-phase separation; and diffusion, flow, and mechanical force for VPS. More specifically, diffusion and flow are driven by osmotic-stress gradients in fluid-phase separation, whereas they are driven by osmotic- and mechanical-stress gradients in VPS. The difference in the transport mechanisms is the origin of the difference in pattern evolution.

The key to VPS is dynamic asymmetry between the two components of the mixture (see Fig. 1). For example, in a polymer solution, the polymer moves much more slowly because its molecules are much larger than the surrounding solvent molecules. This dynamic asymmetry means that the small fast molecules can relax on timescales many orders of magnitudes shorter than large slow molecules. Such “dynamic asymmetry” can be induced by either a large size difference or a large difference in glass-transition temperature ( $T_g$ ) between the components of a mixture. The former often exists in so-called complex fluids and biological systems, including polymer solutions,<sup>[7–11]</sup> colloidal suspensions,<sup>[12–15]</sup> protein solutions,<sup>[16]</sup> surfactant solutions,<sup>[17]</sup> and emulsions.<sup>[18]</sup> The latter, on the other hand, exists in any mixtures, such as oxides and metallic alloys, in principle.<sup>[5,6,19]</sup> Recently, it has been argued that nuclear compartmentalization in a biological cell can be explained by VPS of the dynamically different nuclear components, in

[\*] Prof. Hajime Tanaka  
Institute of Industrial Science  
University of Tokyo  
Komaba 4-6-1, Meguro-ku  
Tokyo 153-8505 (Japan)  
E-mail: tanaka@iis.u-tokyo.ac.jp

**Table 1.** Relationship between the mechanical response of materials for deformation and classification of phase separation.

Criteria for material classification	Observation time $\gg$ relaxation time	Observation time $\approx$ relaxation time	Observation time $\ll$ relaxation time
Type of materials	Liquid	Viscoelastic matter	Solid
Criteria for classification of phase separation	Deformation rate $\ll$ relaxation rate	Deformation rate $\approx$ relaxation rate	Diffusion only
Type of phase separation	Fluid phase separation	Viscoelastic phase separation	Solid phase separation

combination with macromolecular crowding and the properties of colloidal particles.<sup>[3]</sup> Therefore, VPS may also be relevant to pattern formation in biology.

Since the physical mechanism of VPS has already been discussed elsewhere,<sup>[5,6,10]</sup> we mainly discuss how VPS can be applied to Materials Science in this article. There are theoretical studies on viscoelastic effects<sup>[20,21]</sup> and numerical-simulation studies on pattern evolution.<sup>[22]</sup> We refer readers who are interested in these theoretical aspects to the above references. From the point of view of applications, control of the phase-separation morphologies may be central. VPS can produce two types of phase-separation structures, which cannot be formed by normal phase separation: network and cellular structures. Heterogeneous structures, such as cellular (foam) and network patterns, are highly versatile, and used both in nature and industry. The connectivity of the phases is one of the key factors that controls the transport capability and the mechanical

properties of phase-separated structures. For example, network structures of cartilage are mechanically strong despite their light weight, and liquid components (blood) can flow freely in the network structure. These structures are important for various applications, including artificial bones, substrates for cell growth, and filters. In cellular structures, on the other hand, the phase that forms cell walls is interconnected, whereas the other phase (in compartments) is isolated. This situation is quite different from a network structure where both phases are interconnected. Cellular structures are also famous for their extremely high mechanical strength per unit weight; plastic foam and aluminum honeycomb are such examples. In particular, they are much more resistant to volume deformation than network structures. Phase separation is quite useful for producing these heterogeneous structures in industry, since these structures can be formed in a self-organized manner, which simplifies the formation process and saves energy in comparison to a bottom-up method. In order to control

morphology using phase separation, it is very important to understand the basic physical principles behind pattern selection in nonequilibrium processes. Here, we show how a rich variety of phase-separated morphologies—droplet, network, and cellular structures—can be formed using the physical principle of VPS.

## 2. Mechanism and Generality of VPS

### 2.1. Physical Mechanism of VPS

As mentioned above, dynamic asymmetry in a mixture originates from either a large size disparity or a large difference in  $T_g$  between the components of the mixture.<sup>[5,6]</sup> In general, the requirement for the occurrence of VPS is that the phase rich in the slow component has a lower relaxation rate than the characteristic deformation rate induced by phase separation, and it behaves as an elastic body for a certain period of time. Under such conditions, the phase-separation pattern is dominated by the elastic-force balance condition<sup>[5,6,20]</sup>

$$\partial_i[\Pi_{ij} - \sigma_{ij} + p\delta_{ij}] = 0 \quad (1)$$

where  $\Pi_{ij}$  is the osmotic stress,  $p$  is the pressure, and  $\sigma_{ij}$  is the mechanical stress. Here,  $p$  is determined to satisfy the incompressibility

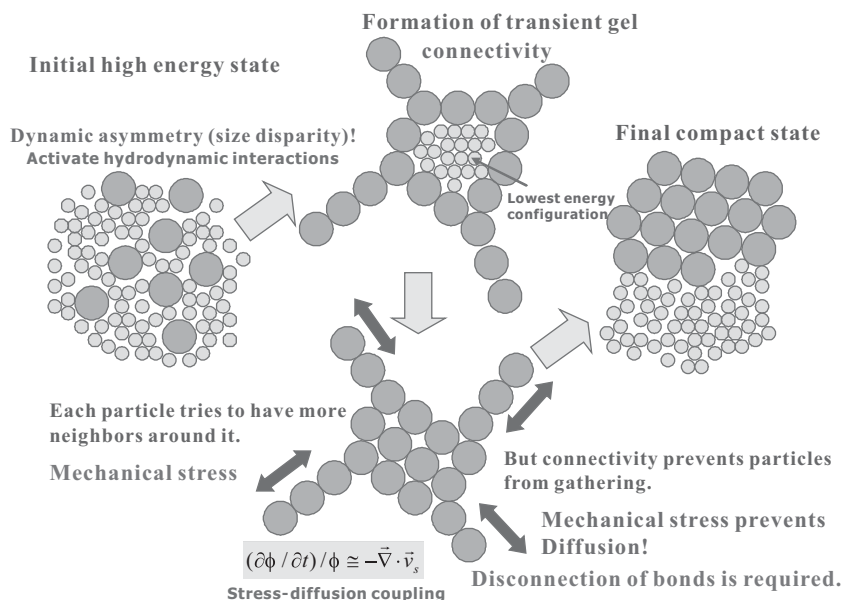


**Figure 1.** Schematic explaining the physical mechanism of VPS in soft matter. Here, big dark gray particles represent slow components, such as polymers, colloids, and proteins, whereas small light gray particles represent solvent molecules. After initiation of phase separation, the small particles can relax very quickly to the lowest-energy configuration. However, once the big particles are connected to form a network structure with the help of hydrodynamic interactions, there is no simple way to relax to the final lowest-energy configuration (the image furthest right). The connectivity prevents the big particles from lowering the contact energy by forming a more compact structure. In other words, the diffusion is prevented by mechanical stress generated by the connectivity: stress-diffusion coupling. This coarsening mechanism can be active even in the absence of thermal noise (even at  $T=0$ ), since it is of a purely mechanical nature [15].

condition.  $\delta_{ij}$  is the Kronecker delta with  $i$  and  $j$  representing one of the Cartesian coordinates  $x$ ,  $y$ ,  $z$ . It is this force-balance condition that controls the network morphology in VPS. This elastic-force balance is a consequence of momentum conservation;<sup>[5,6]</sup> in other words, it stems from the existence of a liquid component.

In soft matter, the formation of a transient gel plays a crucial role in VPS (see Fig. 1). Transient gelation is a consequence of large size disparity between the components of a mixture. It is the connectivity in this transient gel that prevents simple diffusion-dominated phase separation. We emphasize that the viscoelastic properties, or slow relaxation, originate from the connectivity of the transient gel itself. This means that an individual particle needs not have elastic degrees of freedom. This may be the case for colloidal suspensions<sup>[12]</sup> (see Fig. 1 for an intuitive explanation). In polymer solutions, entanglement of the polymer chains further slows the dynamics of the polymer-rich phase.<sup>[23]</sup> As shown in Figure 2a–c, the patterns observed in dilute polymer solutions, protein solutions, and colloidal suspensions and their temporal changes are strikingly similar. This strongly suggests that the network-forming phase separation observed in all these examples should be classified as VPS, irrespective of the origin of dynamic asymmetry. This indicates the generality of VPS in various dynamically asymmetric mixtures.

In a mixture of components with very different  $T_g$ s, the phase rich in the slow component has a lower relaxation rate than the characteristic deformation rate induced by phase separation.<sup>[5,6,19]</sup> This means that dynamic asymmetry always leads to VPS if it is strong enough, irrespective of its origin. This is because in both types of dynamic asymmetry the morphological evolution of VPS is commonly governed by momentum conservation, or the mechanical-force balance condition (Equation 1).

In the final stage of VPS, the system approaches the final equilibrium state, which leads to the slowing down of the coarsening. Thus, the deformation rate decreases with time. Eventually, it becomes even slower than the characteristic rheological time of the phase rich in the slow component. Then the system starts to behave as a liquid rather than as an elastic body (see Table 1). Instead of mechanical stress, interfacial tension starts to dominate the domain morphology. Thus, network or cellular structures become unstable, and relax to droplets or bicontinuous structures. Such behavior can be seen, for example, in Figure 3b. This shows the typical final stage of pattern evolution in VPS. When the phase rich in the slow component is frozen by gelation, vitrification, or ordering during phase separation, the network or cellular structures also freeze. This can be regarded as a special case of VPS, and may provide a novel phase-separation route to gelation for colloidal suspensions and protein solutions.<sup>[13,15,16]</sup> For industrial applications, it is important to stabilize the intermediate phase-separation morphologies, such as network and cellular structures. For this purpose, we can use chemical reactions to arrest VPS in addition to the above-mentioned mechanisms of dynamic arrest.

## 2.2. Difference between VPS and Elastic Phase Separation

Here we discuss the difference in the phase-separation morphologies of elastically asymmetric solid mixtures<sup>[2]</sup> and

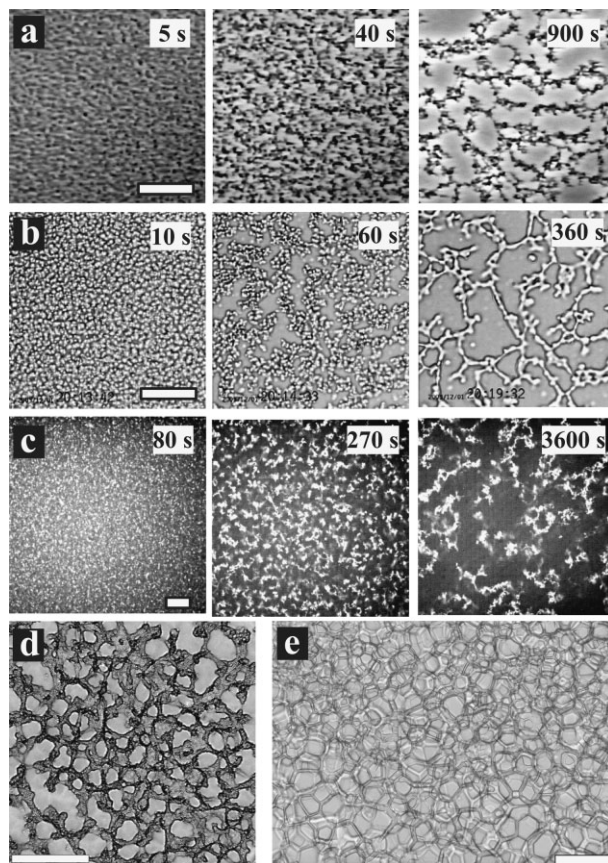


**Figure 2.** Comparison of pattern evolution observed in a) a polymer solution, b) a protein solution, and c) a colloidal suspension. Scale bars in a–c): 50  $\mu\text{m}$ . The image in a) has been observed on a mixture of polystyrene (molecular weight: 706 000) and diethyl malonate (0.5 wt% polystyrene) at temperature,  $T = 20^\circ\text{C}$ , using phase-contrast microscopy. The image in b) was observed on a protein solution (concentration,  $\phi = 200 \text{ mg mL}^{-1}$ , salt (NaCl) concentration 7.5 wt%) at  $37^\circ\text{C}$  using conventional optical microscopy. The image in c) was observed on a colloidal suspension ( $\phi = 0.25 \text{ vol\%}$ , salt (NaCl) concentration 15 wt%) using confocal microscopy. The patterns observed and their temporal changes are strikingly similar. This strongly suggests that VPS may be universal to dynamically asymmetric mixtures. d) Network pattern observed for  $\text{C}_{10}\text{E}_3/\text{H}_2\text{O}$  mixtures (19.9 wt%  $\text{C}_{10}\text{E}_3$ ) at  $42.7^\circ\text{C}$  (5 s after heating at  $6.0 \text{ K min}^{-1}$  was stopped). Scale bar: 500  $\mu\text{m}$ . e) 3D cellular structure observed for a  $\text{C}_{12}\text{E}_5/\text{water}$  mixture of 19.9 wt%  $\text{C}_{12}\text{E}_5$  at  $74.0^\circ\text{C}$ . The sample thickness was 140  $\mu\text{m}$ . Scale bar: 200  $\mu\text{m}$ .

dynamically asymmetric fluid mixtures. In the former, diffusion is the only transport mechanism, whereas in the latter hydrodynamic transport driven by mechanical stress also plays a crucial role. In the former, the system approaches the final equilibrium state to reduce the total free energy, including the elastic energy, since the diffusion is induced by the osmotic-stress gradient. As a result, the morphology that tends to minimize the elastic energy is selected. For example, when a softer phase is the minority phase, it forms a network-like structure, since its deformation costs less energy than that of a harder phase. This is the case of solid mixtures that have only elastic asymmetry but no dynamic asymmetry. Note that phase separation of elastic solid mixtures (such as metal alloys) does not accompany any drastic



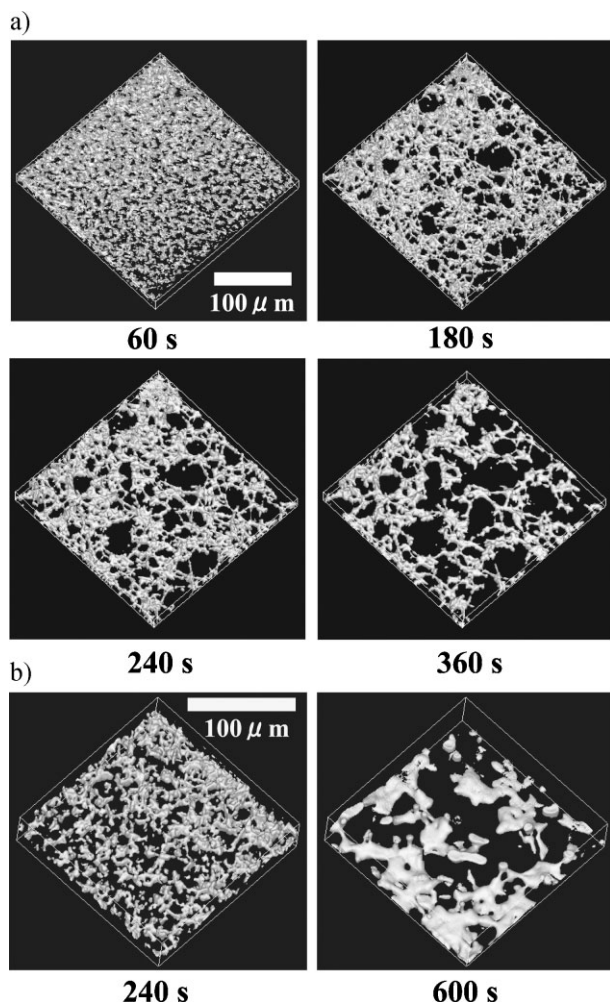


**Figure 3.** Temporal change in 3D phase-separation patterns in protein (lysozyme) solutions. a) Pattern evolution during phase separation observed at 41 °C for a solution containing 150 mg mL<sup>-1</sup> lysozyme and 7.5 wt% NaCl (240 μm × 240 μm × 20 μm). The quench depth measured from the binodal line in this case is 2.5 K. b) Pattern evolution during phase separation observed at 42 °C for  $\phi = 175$  mg mL<sup>-1</sup> and 7.5 wt% NaCl (160 μm × 160 μm × 40 μm). It can clearly be seen that the interface becomes rounded in the final stage. This is the result of viscoelastic relaxation during phase separation [5,6].

volume change of each phase if there is no strong composition dependence of mobility.

In dynamically asymmetric mixtures where transport is dominated by stress-induced flow, on the other hand, the force-balance condition (Equation 1) plays an essential role in pattern selection. As a result, the morphology itself is selected by the force-balance condition. The asymmetric stress division leads to a network structure in which the more viscoelastic phase forms a continuous network structure to support the mechanical stress. Furthermore, the two-fluid nature enables volume change of the phases. It is worth noting that in phase separation of gels the morphology is determined by the force-balance condition and not by the elastic energy in the intermediate stage, even though the gel is elastic and the elastic deformation energy is included in the Hamiltonian. The final structure is, however, determined by

the elastic energy. This is due to the fact that the gel has a fluid component, and thus the force-balance condition plays a crucial role in the selection of the morphology.<sup>[20]</sup>

The two types of morphology-selection mechanisms, that is, selection due to energy minimization and due to momentum conservation,<sup>[5]</sup> can be used to design heterogeneous material structures.

### 3. Various Patterns that can be Produced by VPS

First we discuss the kinds of patterns that can be produced by VPS, and stress that it is not possible for the following patterns to be formed in solid- or fluid-phase separation.

#### 3.1. Formation of Monodisperse Droplets

Monodisperse droplets are quite useful in many applications, particularly in pharmacy and chromatography. They have often been made using rather complex methods, such as successive seeded emulsion polymerization, emulsifier-free polymerization, and dispersion polymerization. There have been reports on a simple method for producing monodisperse polymer particles using phase separation of dilute or semidilute polymer solutions.<sup>[24]</sup> This method is much simpler and straightforward than the previously mentioned conventional techniques. However, its physical mechanism has not yet been clarified. We have proposed that the formation of monodisperse particles can be explained by the physical mechanism that stabilizes the moving droplet phase (MDP), which is one interesting consequence of VPS. The MDP is characterized by the monodispersity of its particles and its unusual stability,<sup>[8–10]</sup> both of which may be necessary conditions to create monodisperse particles from a polymer solution using phase separation.

Here we consider the physical mechanism that prevents droplets from coarsening with time.<sup>[9,10]</sup> The two important time scales characterizing the situation may be the characteristic time of collision between two droplets (or the contact time),  $\tau_c$ , and the characteristic rheological time of the polymer-rich droplet phase,  $\tau_t$ .  $\tau_c$  is primarily controlled by the Brownian motion of droplets.  $\tau_t$  characterizes the time scale of interdiffusion of polymers between two droplets that are in contact. Viscoelastic effects should play a role in phase separation only when  $\tau_c$  is less than or comparable to  $\tau_t$ ; in other words, a droplet may behave as an elastic ball on the collision time scale for  $\tau_t > \tau_c$ . For  $\tau_t < \tau_c$ , on the other hand, droplets can coalesce with each other via the interdiffusion of polymers between the two colliding droplets. This viscoelastic effect is probably responsible for the slow coarsening and the unusual dependence of the coarsening rate on the quench depth.

Since  $\tau_t$  is strongly dependent on the molecular weight of the polymers and the composition of the droplet phase, it is natural that this phase is more stable in solutions of polymers with high molecular weights and/or under deep quench conditions. On increasing  $\tau_t/\tau_c$ , the coarsening rate should decrease, and finally the MDP might be kinetically stabilized for  $\tau_t \gg \tau_c$ . Such complete stabilization behavior was actually observed in mixtures of poly(vinyl methyl ether) and water and of poly(isopropyl acryl amide) and water<sup>[8–10]</sup> for low polymer concentrations under deep

quench conditions. Low polymer concentrations are necessary to avoid percolation of the polymer-rich phase and to produce isolated droplets rather than interconnected-network structures. It should be noted that for these two mixtures there is a possibility that the droplets are in a physical gel state or a glassy state ( $\tau_t = \infty$ ): dynamically arrested droplet spinodal decomposition (or nucleation). The possibility of stabilization due to electrostatic interactions has also been suggested. In such a stable MDP, the size distribution of the droplets is very narrow.<sup>[8–10]</sup> This probably reflects the fact that the droplet size is homogeneous in the initial stage of droplet spinodal decomposition; in other words, the droplet size is selected by the wavelength of the most unstable mode in droplet spinodal decomposition. We note that the evaporation–condensation mechanism<sup>[1,2]</sup> can play only a minor role in the coarsening dynamics of the MDP, since vigorous Brownian motion of the droplet smears out the concentration profile around the droplet in the matrix phase within the timeframe required for diffusion, and thus allows no stationary, directional diffusion field to exist. This is another important factor to consider with regards to coarsening dynamics and stability of the MDP.

We speculate that the physical principle behind the formation of the monodisperse droplets is not limited to polymer solutions, but may be generic to any mixture of a slow, large component and a low-viscosity solvent. Indeed, we have confirmed that the coarsening speed of the droplet phase is unusually slow for protein solutions<sup>[16,25]</sup> and colloidal suspensions.<sup>[13]</sup> The key to droplet stabilization in the above example of the polymer solution is the vigorous Brownian motion of the particles. Thus, the lower-critical-solution-temperature-type (LCST-type) phase diagram and the low viscosity of the solvent may be important in realizing stable MDPs. In addition to the kinetic stabilization mechanism,<sup>[8–10]</sup> electrostatic stabilization may be used to further stabilize the droplets. For practical purposes, perfectly stable droplets have to be prepared, which can be realized by permanent crosslinking via chemical reactions or by vitrification.

### 3.2. Formation of Network Structures of the Minority Phase

#### 3.2.1. Principles Governing the Network Morphology

In the process of VPS, the motion of the domain interface is governed by the force-balance condition (Equation 1).<sup>[5,6,20]</sup> It is this force-balance condition that controls the network morphology. The key deformation mode is  $\nabla \cdot \vec{v}_s$ , where  $\vec{v}_s$  is the averaged local velocity of the slow component, that is, volume shrinking of the phase rich in the slow component. The phase rich in the slow component tends to shrink because of attractive interactions between its components. This situation is basically the same as in volume shrinking of gels.<sup>[2]</sup> This causes mechanical stress if the homogeneous shrinking of the system is prohibited by boundary conditions, or if it is so slow that the stress cannot be relaxed during pattern evolution. The stress is then supported selectively by the slow-component-rich phase due to asymmetric stress division. We emphasize that it is this asymmetric stress division that leads to coupling between the force-balance condition and the topology of the phase-separated structure. The matrix is stretched everywhere as a result of the volume-shrinking tendency. The

force balance in viscoelastic matter determines the morphology and leads to a network structure: in 3D, the stress can be balanced among four arms sharing a junction point in the network. Such 3D structures can be seen in Figure 3, where the network structure is observed by confocal microscopy for phase separation of a protein (lysozyme) solution.<sup>[16]</sup> In 2D, on the other hand, the stress can be balanced among three arms, as can be seen in Figure 2. If an external stress is applied, the structure tends to adjust to satisfy the force-balance condition including external stress. This is a unique and interesting feature of pattern formation due to mechanical selection.

There are a number of examples of network structures in Materials Science that may be explained by the mechanism of VPS. Such examples are mentioned below.

#### 3.2.2. Polymerization-Induced Phase Separation

Polymerization-induced phase separation has recently attracted increasing attention from both fundamental and industrial viewpoints.<sup>[26]</sup> The origin of the phenomenon is very simple. Suppose there is a homogeneous mixture of two liquids. If we initiate the polymerization of one of the components by light or heat, the contribution of the mixing entropy significantly decreases as the polymerization proceeds. Polymerization effects can be included in the theory as a temporal change in the degree of polymerization,  $N$ , of the polymerized component,  $A$ . According to the Flory–Huggins mean-field theory, for example, the mixture may finally become unstable and start to phase separate even at a fixed temperature, since the contribution of the entropy of mixing decreases with increasing  $N$ . It is known that polymerization-induced phase separation often results in network-like or spongelike structures of the minority polymerized phase. The most well-known example are polymer-dispersed liquid-crystal films.<sup>[27–30]</sup> Amundson et al.<sup>[29]</sup> and Nephew et al.<sup>[30]</sup> have used confocal microscopy to reveal 3D network-like and foamlike structures.

The formation of these structures can quite naturally be explained by the mechanism of VPS.<sup>[5,6]</sup> During phase separation, one of the components is polymerized, and thus the resulting asymmetric growth of the molecular size leads to strong dynamic asymmetry between the two components. Thus, pattern evolution in such polymerization-induced phase separation is strongly influenced by viscoelastic effects. Since there is a fluid component in the system, the force-balance condition (Equation 1) determines the morphology, which is different from the case of the elastic solid model (see Section 2.2.). The pattern evolution is first strongly affected by the initial growth of dynamic asymmetry and the resulting VPS. Then the structure becomes frozen if the crosslinking reaction proceeds simultaneously with the linear polymerization. Thus, we believe that the viscoelastic effects dominate the pattern evolution. It is predicted that a more viscoelastic phase, namely, a polymerized phase, forms a network-like or spongelike pattern during polymerization-induced phase separation. Indeed, such a morphology is commonly observed.<sup>[29,30]</sup> Recently, we have confirmed the relevance of this scenario by numerical simulations.<sup>[31]</sup>

#### 3.2.3. Application to Membrane Filters

The formation of membrane filters has been extensively studied for a long time because of their wide applications. In many

cases,<sup>[32]</sup> the final phase-separated patterns prepared as membranes have a morphology that is peculiar to the intermediate stage of VPS. The pattern evolution observed in the process of membrane-filter formation can also be naturally explained by VPS.<sup>[5,6]</sup> Polymeric membranes are often formed from polymer solution by exploiting phase separation. In the membrane-formation process, phase separation of polymer solutions is induced by either evaporating a solvent or replacing a good solvent by a poor one (a wet process). The latter process is used, for example, in the production of viscose fibers. Once phase separation is initiated, viscoelastic effects come into play, and lead to the formation of network-like or spongelike structures of a polymer-rich phase, which is suitable for use as a filter. The structures can then be made permanent by one of the following methods: i) simultaneous evaporation of a solvent for a polymer solution during phase separation, which leads to crystallization or vitrification of the polymers; ii) further quenching of the system below  $T_g$  or the melting point; and iii) including other processes, such as crosslinking reactions. The process of evaporation requires the continuity of the solvent-rich phase, which naturally leads to the formation of network structures rather than cellular structures. With respect to iii), we point out that the above-mentioned polymerization-induced phase separation can also be applied to the formation of membrane filters.

### 3.3. Formation of Cellular Structures

It is well-known that plastic foams have a cellular structure. The formation of foam patterns can be regarded as a special case of VPS. When we consider the force-balance equation (Equation 1) in the formation of network patterns, the pressure,  $p$ , plays only a minor role:  $p$  is determined to satisfy the incompressibility condition. However, the formation of foam structures is usually induced by the liquid-to-gas transformation of one of the components of a mixture (see below), which accompanies its large volume expansion. This expansion creates a high internal pressure, and thus  $p$  plays a crucial role in the morphological selection in foam formation. The force balance can be satisfied only when a gas bubble is surrounded by the matrix phase: the internal gas pressure is balanced by the mechanical stress created by the stretched matrix phase surrounding the gas bubble. It is this feature that leads to the formation of cellular foam structures. As in the case of network formation in VPS, we can say that foam formation is a mechanically selected pattern formation, and thus a special case of VPS.

#### 3.3.1. Plastic Foams: Morphological Selection due to Gas Pressure

A typical formation process of plastic foams is as follows.<sup>[33]</sup> First, a polymer absorbing a low-boiling-point solvent is prepared. Then, its temperature is raised above the boiling point of the solvent, which induces bubble formation in the polymer matrix. These bubbles nucleate and grow from the solvent supplied by the polymer matrix. The total volume of the sample expands as a result of the liquid–gas transformation of the solvent. In this process, the pattern is dominated by the elastic-force-balance condition (Equation 1), as in the case of VPS. This is caused by the strongly asymmetric stress division: gas bubbles cannot support any stress and only the polymeric phase can support mechanical

stress. In this way, a cellular pattern is formed. Recently, the process of polyurethane-foam formation was studied in detail by Mora et al. and Elwell et al.<sup>[34]</sup> In these studies, the process was divided into four main regions: i) bubble nucleation, ii) liquid-foam and microphase separation, iii) physical gelation resulting from vitrification of the hard segment-rich phase, and iv) chemical reaction to yield the foamed copolymer. The process is a bit complicated, but its basic principles are the same as described above. Thus, we argue<sup>[5,6]</sup> that the basic physics behind these phenomena is essentially the same as that of VPS.

In relation to this, it should be mentioned that plastic foams with a periodic, regular structure can be produced using a special preparation method,<sup>[35]</sup> although plastic foams with disordered structures are usually formed by VPS. This may be explained by the nucleation of solvent holes: only when nucleation is heterogeneously induced with a high density in a short period, may a periodic sponge structure be formed as a result of long-range elastic interactions between solvent holes (elastically induced correlated nucleation).

#### 3.3.2. Formation of Stable Foams in Smectic Liquid Crystals: Stabilization of Foams as a Result of Smectic Order

Usually, foam structures are created in a nonequilibrium process, and they coarsen with time. The structures can be stabilized only by some solidification mechanism. Here, we show a novel method to form a stable foam structure using smectic ordering of the matrix phase. We have recently successfully produced such stable foam structures in surfactant solutions ( $C_{10}E_3$ (triethyleneglycol mono n-decyl ether)/ $H_2O$  and  $C_{12}E_5$ (pentaethyleneglycol mono n-dodecyl ether)/ $H_2O$  mixtures) that have a lamellar (smectic) order.<sup>[17]</sup> In this system, three types of morphologies can be produced solely by changing the heating rate: cellular, network, and droplet structures (see the literature<sup>[17]</sup> for the phase diagram of the system). Examples of network and cellular structures formed via the phase separation of a lamellar phase into a lamellar and a sponge phase are shown in Figure 2d and e, respectively.<sup>[17]</sup> We have demonstrated that the kinetic interplay between phase separation and smectic ordering is the key to morphological selection. This may provide a novel route to forming network and stable cellular morphologies in soft materials.

Cellular phase separation is a quasiequilibrium process in the sense that it is realized when the phase transformation can follow the phase-volume change induced by the heating rate. Under such quasiequilibrium conditions, the local mechanical-force-balance condition can be satisfied; that is, the cellular structure is stabilized by elastic constraints of the lamellar smectic order. This elastic-force balance provides the stability of the structure against thermal fluctuations (see the literature<sup>[17]</sup> for the detailed mechanism of stabilization).

We emphasize that the formation of this type of foam structure is markedly different from that known for soap froth<sup>[36]</sup> and plastic foam (Section 3.3.1.). In soap froth, for example, the rearrangement of walls driven by gas diffusion dominates coarsening,<sup>[36]</sup> and the structure coarsens indefinitely obeying a power law. In “breaking” foam, in which rupturing of the walls occurs in addition to the rearrangement, the cell-size distribution becomes very broad, and this heterogeneous structure further coarsens indefinitely. On the other hand, the coarsening of the



cellular structure in membranes is promoted by the decrease in the volume fraction of the lamella phase. We stress that the structure itself is stabilized by elastic constraints of the lamella smectic order at constant temperature. We may say that the structure is mechanically optimized to satisfy the elastic-force-balance condition. In short, the cellular structure with smectic order is stable and rather homogeneous, whereas the structures of soap froth and plastic foam coarsen indefinitely and have to be frozen to stop coarsening.

Finally, we note that our method may be applied in a straightforward manner to the phase separation of systems with smectic order, such as thermotropic smectic liquid crystals and block copolymers. The basic physical strategy may also be used for various types of soft matter that have other internal order and that can support elastic stress, which may open a new route to obtaining a variety of stabilized foam structures.

## 4. Beyond Soft Materials

Here we consider the relevance of VPS to hard materials, such as mixtures of metals, semiconductors, and oxide glasses. One obvious way to make hard materials with network and cellular structures is via soft materials: After forming network or cellular structures using VPS of soft matter, they could be heated to temperatures high enough to remove residual organics. The remaining inorganic components may maintain the original structures. This method is often used for making inorganic network structures from silica or carbon (see, for example, sol-gel methods<sup>[31k]</sup>). Since this method is basically the same as that used for soft materials except for the final heating process, we propose other plausible routes.

### 4.1. Phase-Separation Approach

We may produce network and cellular structures using phase separation, as in VPS, of soft matter. There are a number of systems such as  $\text{SiO}_2/\text{Na}_2\text{O}$ , semiconductor mixtures, and metallic glass formers, which have a thermodynamic phase diagram associated with demixing. If  $T_g$  is very different between the components of a mixture, the same principle of VPS in soft matter can be applied. Even a minority phase should form a network structure in phase separation, if we choose proper conditions under which the deformation rate of phase separation exceeds the structural relaxation rate of the phase rich in the slow component. For example, we expect that for a  $\text{SiO}_2/\text{Na}_2\text{O}$  mixture, the network structure of the  $\text{SiO}_2$ -rich phase (the phase rich in the high- $T_g$  component) may be formed by phase separation even if it is the minority phase. This strategy may also be used for bulk metallic-glass formers, which are multi-component atomic mixtures and often display phase separation near  $T_g$ .<sup>[37]</sup>

### 4.2. Colloidal Approach

Another possibility to induce dynamic asymmetry to hard matter is to use solid particles made of hard materials such as metals, semiconductors, and oxide glasses as colloids.<sup>[38]</sup> After suspend-

ing these particles in liquids, VPS can be induced by introducing strong attractive interactions between solid particles, for example by adding polymers to colloidal suspensions (depletion attraction). If the effect of density mismatch and the resulting sedimentation are not so severe, then a network structure composed of these particles can be formed, as shown in Figure 2c. To avoid sedimentation effects, it may be important to use very small particles. This method may open up a new way to produce network structures of hard-matter particles with electronic or optical functions. We can also use wetting effects to produce such structures (see the literature<sup>[39]</sup> for details). For optical applications, structural formation of colloids acting as quantum dots (nanoparticles of semiconductors) may also be quite interesting.

### 4.3. Foam Approach

The same principle used in plastic foams can also be used. Recently, such procedures were applied to make metallic foams using bulk metallic-glass formers.<sup>[40]</sup> Typically, molten metals with adjusted viscosities are prepared. Melts can then be foamed by injecting gases or by adding gas-releasing blowing agents that decompose in situ, causing the formation of bubbles. Unique properties of foams include high strength/weight ratio, high impact-energy absorption, and good thermal insulation. Thus, metallic foams should become an attractive research topic both from the scientific and industrial viewpoints. For such applications, highly viscous metallic liquids, whose structural relaxation time is comparable to the deformation rate induced by bubble growth, are needed. In this sense, bulk metallic-glass formers, whose supercooled liquid state exhibit extreme stability (against crystallization), are one of the best materials for foam formation. Other glassy liquids, such as oxides, may also be used. The difference in the mechanical behavior between plastic, metallic, and oxide glasses adds to the variety of foams that can be produced.

## 5. Other Topics: Food Science, Photonic Devices, Cracks

The formation of network and cellular structures is also very important in food science.<sup>[41]</sup> The structures are closely related to the elasticity felt when they are being eaten. An example of foam formation that can be found in daily life is bread.<sup>[42]</sup> A diverse range of foods are aerated using a similarly varied assortment of processing methods. VPS allows the design of structures of various foods using phase-separation processes, including gas-bubble formation, as in the bread-making process.

Another interesting possible application is the so-called photonic amorphous, which has recently been found to have an optical band-gap despite the absence of periodicity.<sup>[43]</sup> The amorphous structure is characterized by local tetrahedral (diamond-like) order, whose symmetry is similar to that preferred by VPS. As noted above, the force-balance condition (Equation 1) favors a 3D network structure with four-arm junctions. This structure may allow the optical electric field to have the incompressible vector field that satisfies the Maxwell equation. To render the structure photonic active, a high-refractive-index

network (with an index as high as that of Si or Ge) are needed, which can be made using strategies discussed in Section 4. The avoidance of defects (disconnection of the network) may be crucial in such applications.

Finally, we briefly mention fracture phase separation, which we have very recently discovered.<sup>[44]</sup> When the deformation rate produced by phase separation becomes much higher than the structural relaxation rate of the slow components, the system starts to behave like an elastic solid, and phase separation proceeds with accompanying mechanical fracture (see Table 1). The transformation from VPS to fracture phase separation can be viewed as the transformation from ductile to brittle fracture. This change in the type of phase separation resulting from the crossover between the deformation and relaxation rates resembles mechanical instability under shear deformation.<sup>[45]</sup> This phenomenon also has a link to the formation of shrinkage-crack patterns, which is a ubiquitous phenomena commonly observed in Nature (tectonic plates, dried mud layers, and cracks on rocks) and in man-made materials (concrete, ceramic glaze, glass, and coatings).<sup>[46]</sup> They appear in materials that contract upon cooling or drying: mechanical instability associated with volume (area) shrinking. Thus, VPS can also provide the physical basis for such phenomena as well as fracture behavior of disordered materials. This may allow the design of materials (such as concrete and coatings) in which such surface cracking is absent.

## 6. Conclusions

We have described here how VPS can be applied to the morphological control of materials including soft matter, biological materials, food, and hard matter. In particular, we have shown that VPS can produce two types of phase-separation structures, network and cellular structures, which cannot be formed by normal phase separation. Physical understanding of viscoelastic and elastic effects on phase separation allows the production of a rich variety of morphologies that have not yet been possible. So far, the study of VPS has been performed mainly for elucidating the physical mechanism of structure formation and the role of momentum conservation in the selection of patterns. We hope that the physical principle of VPS will be widely applied for the control of structures of various types of materials.

## Acknowledgements

We thank T. Koyama, Y. Iwashita, Y. Nishikawa, Y. Nakanishi for their collaboration on the experimental studies on VPS and T. Araki for his collaboration on the numerical-simulation studies. This work was partly supported by a grant-in-aid from the Ministry of Education, Culture, Sports, Science and Technology, Japan.

Published online: February 23, 2009

[1] J. D. Gunton, M. San Miguel, P. Sahni, in *Phase Transition and Critical Phenomena*, Vol. 8 (Eds: C. Domb, J. H. Lebowitz), Academic, New York 1983.

- [2] A. Onuki, *Phase Transition Dynamics*, Cambridge Univ. Press, Cambridge 2002.
- [3] F.-J. Iborra, *Theor. Biol. Med. Model.* **2007**, 4, 15.
- [4] R. Voituriez, J.-F. Joanny, J. Prost, *Phys. Rev. Lett.* **2006**, 96, 028102.
- [5] H. Tanaka, *J. Phys.: Condens. Matter* **2000**, 12, R207.
- [6] H. Tanaka, T. Araki, *Chem. Eng. Sci.* **2006**, 61, 2108.
- [7] H. Tanaka, *Phys. Rev. Lett.* **1993**, 71, 3158.
- [8] H. Tanaka, T. Nishi, *Jpn. J. Appl. Phys.* **1988**, 27, L1787.
- [9] H. Tanaka, *Macromolecules* **1992**, 25, 6377.
- [10] H. Tanaka, *J. Chem. Phys.* **1994**, 100, 5323.
- [11] T. Koyama, H. Tanaka, *Europhys. Lett.* **2007**, 80, 68002.
- [12] H. Tanaka, *Phys. Rev. E* **1999**, 59, 6842.
- [13] H. Tanaka, Y. Nishikawa, T. Koyama, *J. Phys.: Condens. Matter* **2005**, 17, L143.
- [14] A. Shalkevich, A. Stradner, S. K. Bhat, F. Muller, P. Schurtenberger, *Langmuir* **2007**, 23, 3570.
- [15] H. Tanaka, T. Araki, *Europhys. Lett.* **2007**, 79, 58003.
- [16] H. Tanaka, Y. Nishikawa, *Phys. Rev. Lett.* **2005**, 95, 078103.
- [17] Y. Iwashita, H. Tanaka, *Nat. Mater.* **2006**, 5, 147.
- [18] T. Moschakis, B. S. Murray, E. Dickinson, *J. Colloid. Interface Sci.* **2005**, 284, 714.
- [19] H. Tanaka, *Phys. Rev. Lett.* **1996**, 76, 787.
- [20] H. Tanaka, *Phys. Rev. E* **1997**, 56, 4451.
- [21] A. Onuki, T. Taniguchi, *J. Chem. Phys.* **1997**, 106, 5761.
- [22] a) T. Taniguchi, A. Onuki, *Phys. Rev. Lett.* **1996**, 77, 4910. b) H. Tanaka, T. Araki, *Phys. Rev. Lett.* **1997**, 78, 4966. c) T. Araki, H. Tanaka, *Macromolecules* **2001**, 34, 1953. d) J. N. Zhan, Z. L. Zhang, H. D. Zhang, Y. L. Yang, *Phys. Rev. E* **2001**, 64, 051510.
- [23] M. Doi, A. Onuki, *J. Phys. II* **1993**, 2, 1631.
- [24] a) B. M. Siegel, D. H. Johnson, H. Mark, *J. Polym. Sci.* **1950**, 5, 111. b) H. R. Brown, *Macromolecules* **1990**, 23, 683. c) W.-H. Hou, T. B. Lloyd, *J. Appl. Polym. Sci.* **1992**, 45, 1783. d) C. Wu, W. Li, X. X. Zhu, *Macromolecules* **2004**, 37, 4989. e) Y. Matsuda, Y. Miyazaki, S. Sugihara, S. Aoshima, K. Saito, T. Sato, *J. Polym. Sci., Part B: Polym. Phys.* **2005**, 43, 2937. f) P. Kujawa, F. Tanaka, F. M. Winnik, *Macromolecules* **2006**, 39, 3048. g) Y. Matsushita, H. Furukawa, M. Okada, *Phys. Rev. E* **2004**, 70, 040501(R).
- [25] H. Sedgwick, K. Kroy, A. Salonen, M. B. Robertson, S. U. Egelhaaf, W. C. K. Poon, *Euro. Phys. J. E* **2005**, 16, 77.
- [26] a) L. A. Utracki, *Polymer Alloys and Blends. Thermodynamics and Rheology*, Hanser, Munich **1990**. b) B. S. Kim, T. Chiba, T. Inoue, *Polymer* **1995**, 36, 43. c) M. Yamazaki, M. Kayama, K. Ikeda, T. Alii, S. Ichihara, *Carbon* **2004**, 42, 1641. d) Y. Yu, M. Wang, W. Gan, Q. Tao, S. Li, *J. Phys. Chem. B* **2004**, 108, 6208.
- [27] P. C. Drzaic, *Liquid Crystal Dispersions*, World Science, Singapore **1995**.
- [28] A. J. Lovinger, K. Amundson, D. D. Davis, *Chem. Mater.* **1994**, 6, 1726.
- [29] K. Amundson, A. van Blaaderen, P. Wiltzius, *Phys. Rev. E* **1997**, 55, 1646.
- [30] J. B. Nephew, T. C. Nihei, S. A. Carter, *Phys. Rev. Lett.* **1998**, 80, 3276.
- [31] H. Nakazawa, S. Fujinami, M. Motoyama, T. Ohta, T. Araki, H. Tanaka, T. Fujisawa, H. Nakada, M. Hayashi, M. Aizawa, *Comput. Theor. Polymer Sci.* **2001**, 11, 445.
- [32] a) J. G. Wijmans, J. Kant, M. H. V. Mulder, *Polymer* **1985**, 26, 1539. b) G. E. Gaides, A. J. McHugh, *Polymer* **1989**, 30, 2118. c) J. H. Aubert, *Macromolecules* **1990**, 23, 1446. d) C. L. Jackson, M. T. Shaw, *Polymer* **1990**, 31, 1070. e) S. W. Song, M. Torkelson, *Macromolecules* **1994**, 27, 6390. f) H. J. Kim, A. Tabe-Mohammadi, A. Kumar, A. E. Foulda, *J. Membr. Sci.* **1999**, 161, 229. g) H. Matsuyama, S. Berghmans, D. R. Lloyd, *J. Membr. Sci.* **1998**, 142, 213. h) H. J. Lee, B. Junga, Y. S. Kanga, H. Lee, *J. Membr. Sci.* **2004**, 245, 103. i) S. S. Prakash, L. F. Francis, L. E. Scriven, *J. Membr. Sci.* **2006**, 283, 328. j) K. Hosoya, N. Hira, K. Yamamoto, M. Nishimura, N. Tanaka, *Anal. Chem.* **2006**, 78, 5729. k) H. Saito, K. Nakanishi, K. Hirao, H. Jinnai, *J. Chromatogr. A* **2006**, 1119, 95. l) C. J. Gommers, M. Basiura, B. Goderis, J.-P. Pirard, S. Blacher, *J. Phys. Chem. B* **2006**, 110, 7757.
- [33] J. J. Crevecoeur, J. F. Coolegem, L. Nelissen, P. J. Lemstra, *Polymer* **1999**, 40, 3697.
- [34] a) E. Mora, L. D. Artavia, C. W. Macosko, *J. Rheol.* **1991**, 35, 921. b) M. J. Elwell, A. J. Ryan, S. Mortimer, *Macromolecules* **1994**, 27, 5428. c) M. J.



- Elwell, A. J. Ryan, H. J. M. Grunbauer, H. C. van Lieshout, *Macromolecules* **1996**, 29, 2960.
- [35] G. Widawski, M. Rawiso, B. Francois, *Nature* **1994**, 369, 387.
- [36] D. Weaire, S. Hutzler, *The Physics of Foam*, Oxford University Press, Oxford **1999**.
- [37] J. F. Löffler, *Intermetallics* **2003**, 11, 529.
- [38] E. Rabani, D. R. Reichman, P. L. Geissler, L. E. Brus, *Nature* **2003**, 426, 271.
- [39] H. Tanaka, *J. Phys.: Condens. Matter* **2001**, 13, 4637.
- [40] a) L. J. Gibson, M. F. Ashby, *Cellular Solids, Structure and Properties*, Pergamon Press, Oxford **1988**. b) J. Banhart, *Prog. Mater. Sci.* **2001**, 46, 559. c) A. E. Simone, L. J. Gibson, *Acta Mater.* **1998**, 46, 3109. d) L. J. Gibson, *Annu. Rev. Mater. Sci.* **2000**, 30, 191.
- [41] R. Mezzenga, P. Schurtenberger, A. Burbidge, M. Michel, *Nat. Mater.* **2005**, 4, 729.
- [42] a) G. M. Campbell, E. Mougeot, *Trends Food Sci. Technol.* **1999**, 10, 283. b) B. J. Dobraszczyk, M. Morgenstern, *J. Cereal Sci.* **2003**, 38, 229.
- [43] K. Edagawa, S. Kanoko, M. Notomi, *Phys. Rev. Lett.* **2008**, 100, 013901.
- [44] T. Koyama, T. Araki, H. Tanaka, *Phys. Rev. Lett.* **2009**, 102, 065701.
- [45] A. Furukawa, H. Tanaka, *Nature* **2006**, 443, 434.
- [46] a) A. Skjeltorp, P. Meakin, *Nature* **1988**, 335, 424. b) A. Groisman, E. Kaplan, *Europhys. Lett.* **1994**, 25, 415. c) K. Shorlin, J. M. G. de Bruyn, S. Morris, *Phys. Rev. E* **2000**, 61, 6950.